Individual and Combined Influences of ENSO and the Indian Ocean Dipole on the Indian Summer Monsoon

KARUMURI ASHOK AND ZHAOYONG GUAN*

Frontier Research Center for Global Change, JAMSTEC, Yokohama, Japan

N. H. SAJI

International Pacific Research Center, University of Hawaii at Manoa, Honolulu, Hawaii

TOSHIO YAMAGATA

Frontier Research Center for Global Change, JAMSTEC, Yokohama, and Department of Earth and Planetary Science, Graduate School of Science, University of Tokyo, Tokyo, Japan

(Manuscript received 27 February 2003, in final form 12 February 2004)

ABSTRACT

The relative influences of the ENSO and Indian Ocean Dipole (IOD) events on the Indian summer rainfall were studied using observational data and an atmospheric general circulation model (AGCM). The composite analysis of rainfall anomalies demonstrates that the IOD, while significantly influencing the Indian summer monsoon rainfall, also significantly reduces the impact of ENSO on the Indian summer rainfall whenever these events with the same phase co-occur.

The AGCM experiments have shown that during an El Niño event, the Walker circulation over the tropical Indo–Pacific region is modulated; a low-level anomalous divergence center over the western Pacific and an anomalous convergence zone over the equatorial Indian Ocean are induced. Furthermore, an anomalous zone of convergence over the Myanmar and south China regions is induced during an El Niño event. These zones of anomalous convergence are complemented by anomalous divergence over the Indian region, causing anomalous subsidence and weakened rainfall. When a strong positive IOD event simultaneously occurs with El Niño, the latter's influence on the Indian monsoon is reduced by both poles of the IOD through the following mechanism: an anomalous divergence center, as compared to the summers when an El Niño alone occurs, is introduced in the eastern tropical Indian Ocean. From this center, the anomalous divergent flow crosses the equator, and this air, while weakening the El Niño–induced divergence over the western Pacific, also leads to convergence over the Indian monsoon region. This results in the reduction of the ENSO-induced subsidence and the related rainfall deficit over the eastern flank of the Indian monsoon trough region and adjoining regions to the east. On the other hand, over the western part of the tropical Indian Ocean sector, part of the anomalous ascending motion from the warm pole of the positive IOD event subsides just to the north of the equator, moves northward, ascends, and causes surplus rainfall. This reduces the ENSO-induced rainfall deficit over western India, the western part of the monsoon trough, and parts of Pakistan. The AGCM experiments also demonstrate that positive IOD events amplify the ENSO-induced dryness over the Indonesian region.

1. Introduction

With a population of about one billion, India mainly depends on the rain-fed agriculture for food grains. Seventy percent of the annual rainfall over India comes from the monsoon rains during the summer: June–September (JJAS). Hence, to satisfy the societal and economic needs of India, the correct seasonal forecasting of the Indian summer monsoon rainfall (ISMR) is very important. A proper understanding of how the different external forcings modulate the Indian monsoon is very useful to achieve this goal.

There are many works on the long-range forecasting studies over India (see Krishna Kumar et al. 1995; Pant and Rupa Kumar 1997; Webster et al. 1998 for details). From this literature, it can be understood that until the late 1980s the El Niño influenced the ISMR extensively. Various indices of El Niño, such as the Southern Oscillation index, have been used in the seasonal prediction of the Indian summer monsoon by many researchers as

* Current affiliation: Nanjing Institute of Meteorology, Nanjing, China.

Corresponding author address: Dr. Karumuri Ashok, Frontier Research Center for Global Change, JAMSTEC, 3173-25 Showa-machi, Kanazawa-ku, Yokohama, Kanagawa 236-0001, Japan.
E-mail: ashok@jamstec.go.jp

well as the India Meteorological Department (IMD). But, in recent years, ENSO has lost its impact on the Indian summer monsoon (Krishna Kumar et al. 1999; Kripalani and Kulkarni 1999). Though there were protracted and intense ENSO events in the 1990s, the ISMR was always normal.[1] In a recent study, Ashok et al. (2001) discovered that there are apparent complementary interdecadal changes between the ENSO–ISMR and Indian Ocean Dipole (IOD)–ISMR relationships. They conclude that the frequent occurrence of IOD events (Saji et al. 1999; Webster et al. 1999) is the cause for the weakening of the relationship between the ISMR and ENSO. From some atmospheric general circulation model (AGCM) sensitivity experiments, Ashok et al. (2001), in agreement with Behera et al. (1999), infer that the IOD phenomenon modulates the meridional circulation by inducing anomalous convergence (divergence) patterns over the Bay of Bengal during positive (negative) IOD events, leading to excessive (deficit) monsoon rainfall over the monsoon trough region.[2] They further conjecture from observations that during the years, such as 1997, when the ENSO co-occurred with the positive phase of the IOD, the ENSO-induced anomalous subsidence is neutralized/reduced by the anomalous IOD-induced convergence over the Bay of Bengal.

The primary objective of the present paper is to demonstrate by use of an AGCM that the IOD can reduce the ENSO-induced influence over the Indian region and to understand the dynamics behind this. In our previous study (Ashok et al. 2001), we reported the AGCM studies for stand-alone IOD cases without any incorporation of the ENSO influence. In this paper we extend the scope of our studies by incorporating the ENSO-related AGCM experiments. Using an AGCM, we examine the relative influences of the IOD and ENSO, as well as their combined influence, on the ISMR. In our earlier paper (Ashok et al. 2001) we only discussed the influence of the eastern pole of the IOD on the Indian summer monsoon. In the present study, we demonstrate that both poles of the positive IOD reduce the influence of the co-occurring El Niño.

Along with the AGCM experiments, we also examine, using the composite analysis, the distribution of observed summer rainfall anomalies over the Indian region during the ENSO years, IOD years, and years in which they co-occur with the same phase (i.e., El Niño event with a positive IOD event or La Niña event with a negative IOD event).

The paper has been divided into the following sections: The second section describes details of the datasets used, as well as the analysis method. We also present in this section a brief description of the AGCM that has been employed to carry out the sensitivity experiments in this study. Section 3 describes the results from the AGCM experiments. In the final section, we present our conclusions along with some discussion.

2. Data, AGCM description, and methodology

a. Datasets used in the study

In the experiments carried out by the atmospheric general circulation model (AGCM), the GISST data from 1958 to 1997 (Rayner et al. 1996) has been used to obtain the lower boundary conditions. SIGRID (gridded sea ice information), compiled at the Joint Ice Center (T. Thompson 1981, unpublished manuscript) has been adopted for the sea ice distribution. The ozone density is from the distribution of Klenk et al (1983). The National Centers for Environmental Prediction–National Center for Atmospheric Research (NCEP–NCAR) reanalysis wind data from 1948 to 1997 (Kalnay et al. 1996) have been used to show some observed circulation features. In our study, the Niño-3 sea surface temperature anomaly[3] (SSTA) and the Indian Ocean Dipole mode index[4] (IODMI; Saji et al. 1999) have been used as the indicators for ENSO and IOD, respectively; these indices have been derived from the GISST data for 1958–97 (Rayner et al. 1996). We use these indices to obtain, by composite analysis, the different SSTA that have been used as lower boundary conditions in our AGCM sensitivity experiments. The land rainfall datasets from the gridded products ($0.5° \times 0.5°$) of Willmott and Matsuaara (1995) have also been used in this study for composite analysis. These land rainfall data have been derived from the Global Historical Climatology Network (GHCN) version 2 and station records of monthly and annual total precipitation (Legates and Willmott 1990).

b. AGCM experiments: Brief description of the AGCM and experimental design

The Frontier Atmospheric General Circulation Model version 1.0 (FrAM1.0; Guan et al. 2000; Ashok et al. 2001; Guan et al. 2003; Ashok et al. 2003b) has been used in this study. In our earlier studies, this model successfully simulated the observed influence of the IOD on the tropical Indian Ocean region and the Indian region. Briefly described, the FrAM1.0 is an AGCM with a horizontal resolution of T42. The vertical domain is divided into 28 layers from the earth's surface up to 10 hPa. A hybrid vertical coordinate system has been employed (Laprise and Girard 1990). Some important features of the model physics are cumulus convection

[1] According to the IMD, the ISMR is normal when the monsoon rainfall anomaly is within ±10% of its seasonal mean.

[2] The location of the line around which the monsoon sea level pressure trough is distributed (as in Fig. 2.2 of Rao 1976) is shown in Fig. 1b.

[3] Area-averaged sea surface temperature anomalies over 5°N–5°S, 150°–90°W.

[4] SSTA difference between the tropical western Indian Ocean (10°S–10°N, 50°–70°E) and the tropical southeastern Indian Ocean (10°S–0°, 90°–110°E).

(Kuo 1974), large-scale condensation, longwave radiation (Shibata and Aoki 1989; Shibata 1989), land surface model (Vitebro and Beljaars 1995), surface fluxes (Mellor and Yamada 1974), and gravity wave drag (Palmer et al. 1986).

Four experiments have been performed in this study, each experiment comprising five member ensembles that differ from each other in initial conditions. The same set of initial conditions was used for all experiments. Each integration lasts for a calendar year, starting from 1 January. The first experiment, henceforth referred to as the control experiment, has been forced with seasonally varying climatological sea surface temperatures (SSTs) as the lower boundary condition. To obtain the lower boundary SST condition for the second experiment, we impose the canonical El Niño–type of SST anomalies obtained by using the composite analysis on these climatological SSTs. These anomalies are obtained in a two-step process: (i) a composite value of the monthly Niño-3 index is obtained by averaging it over pure[5] El Niño years of 1965, 1969, 1976, 1986, 1987, and 1991; and (ii) this composite Niño-3 index is multiplied with the correlation coefficients between the SSTA and Niño-3 index at every grid point. This experiment is referred to as the ENSO experiment. The anomalies imposed during the month of September are shown in Fig. 1a as an example. As the most dominant relationship between the ENSO and summer monsoon rainfall appears to be simultaneous (see Fig. 6.5 of Parthasarathy et al. 1993; also p. 160 of Plant and Rupa Kumar 1997), we design the SSTA of the ENSO experiment so as to mimic the developmental phase of the El Niño (i.e., during the summer of the year by the end of which the warm anomalies in the eastern Pacific peak). The ENSO anomalies are imposed from January. The amplitude of the anomalies is weak in January; it gradually increases and reaches its peak value in December, as observed. We have carried out the third experiment, referred to as the IOD experiment, by imposing positive IOD-type of SSTA on the climatological SSTs. These IOD anomalies, imposed from April, are also canonical in nature. The IOD anomalies, confined to the tropical Indian Ocean, have been obtained in an analogous fashion by averaging the monthly IODMI over the pure positive IOD years of 1961, 1967, 1976, and 1994 and multiplying this monthly composite IODMI with the correlations between the IODMI and the SSTA at every grid point in the tropical Indian Ocean; anomalies so obtained are magnified so as to represent strong positive IOD events such as during 1961, 1994, etc. Just as in our earlier studies (Ashok et al. 2001; Guan et al. 2003; Ashok et al. 2003b), the amplitude of the imposed IOD type SSTA gradually amplifies and reaches its peak in October, in agreement with observations (see Fig. 3 of Saji et al. 1999). As an example, the anomalies imposed during the month of September are shown in Fig. 1b. To carry out the final experiment, the lower boundary SSTs were obtained by imposing a combination of the aforementioned ENSO SSTA and the positive IOD type SSTA together on the climatological SSTs (Fig. 1c). We refer to this final experiment as the combined experiment. The results presented in this paper for each experiment are the average of the simulations from its five member ensembles for the JJAS season. The anomalies of parameters such as rainfall from the ENSO experiment are obtained by subtracting the control experiment simulations from the ENSO experiment simulations. The procedure to obtain anomalies is similar in the case of the IOD experiment. It should also be noted that in the ensuing discussion, the anomalous difference in any parameter between the combined and the ENSO experiments is obtained by subtracting the parameter simulated in the ENSO experiment from that in the combined experiment; that is, for any parameter A:

$$\Delta A = A_{\text{combined}} - A_{\text{ENSO}}.$$

The surplus and deficit quantities presented are relative to the ENSO experiment.

3. Results

a. The relative influences of the ENSO and the IOD events on the Indian summer monsoon rainfall

We have made a composite of the ISMR anomaly distribution during all the El Niño years (including those events that co-occurred with positive IOD events) between 1958 and 1997: namely, 1963, 1965, 1969, 1972, 1976, 1982, 1983, 1986, 1987, 1991, and 1997 (Fig. 2a). Strong negative rainfall anomalies[6] can be seen all over the Indian region. In Fig. 2b, we show the difference in the composite ISMR anomalies between all El Niño years (1965, 1969, 1976, 1986, 1987, and 1991). The sign of the difference is positive over many parts of peninsular India, monsoon trough region, northern India, and parts of Pakistan, demonstrating that the co-occurring positive IOD events have reduced the El Niño–induced rainfall deficit over many parts of Indian subcontinent, as hypothesized in our earlier study (Ashok et al. 2001).

To examine the influence of the pure positive IOD events on the Indian summer monsoon rainfall, we made a composite of the ISMR anomalies from the pure positive IOD years of 1961, 1967, 1977, and 1994 (Fig. 2c). In this figure, significant positive rainfall anomalies

[5] A pure El Niño (positive IOD) year is a year when there is no co-occurring positive IOD (El Niño) event. Similarly, a pure La Niña (negative IOD) year is a year when there is no co-occurring negative IOD (La Niña) event. For further details, please see Rao et al. (2002), Ashok et al. (2003a), and Yamagata et al. (2003).

[6] Student's two-tailed t tests have been applied to identify the significant (at 90% confidence level) rainfall anomalies and significant differences in Figs. 2 and 3.

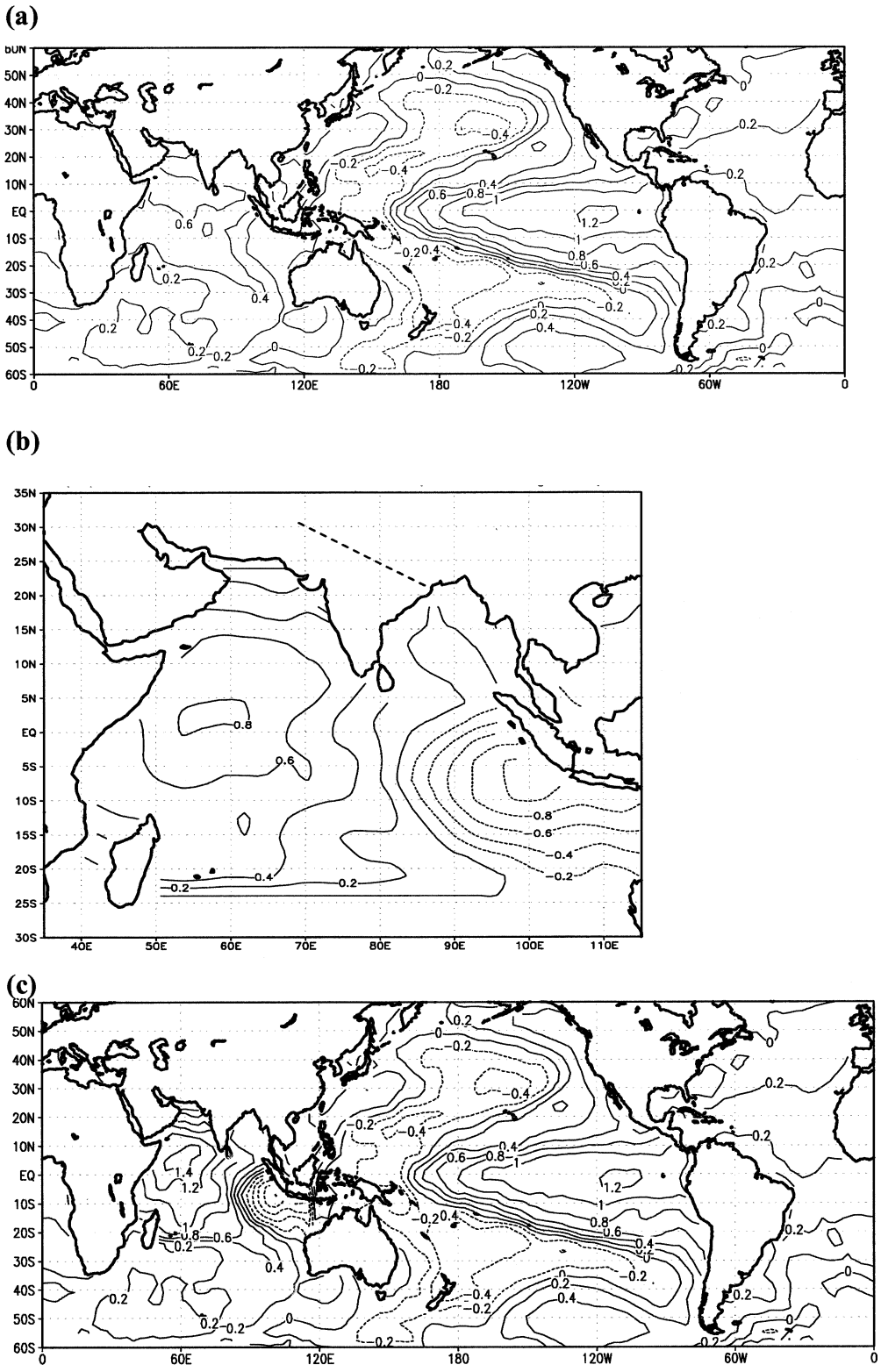

FIG. 1. Sep SSTA (°C) imposed in (a) the ENSO experiment, (b) the IOD experiment, and (c) the combined experiment. The dashed line over the Indian region shown in (b) indicates the mean climatological position of the monsoon sea level pressure trough during July (from Rao 1976, Fig. 2.2, p. 4).

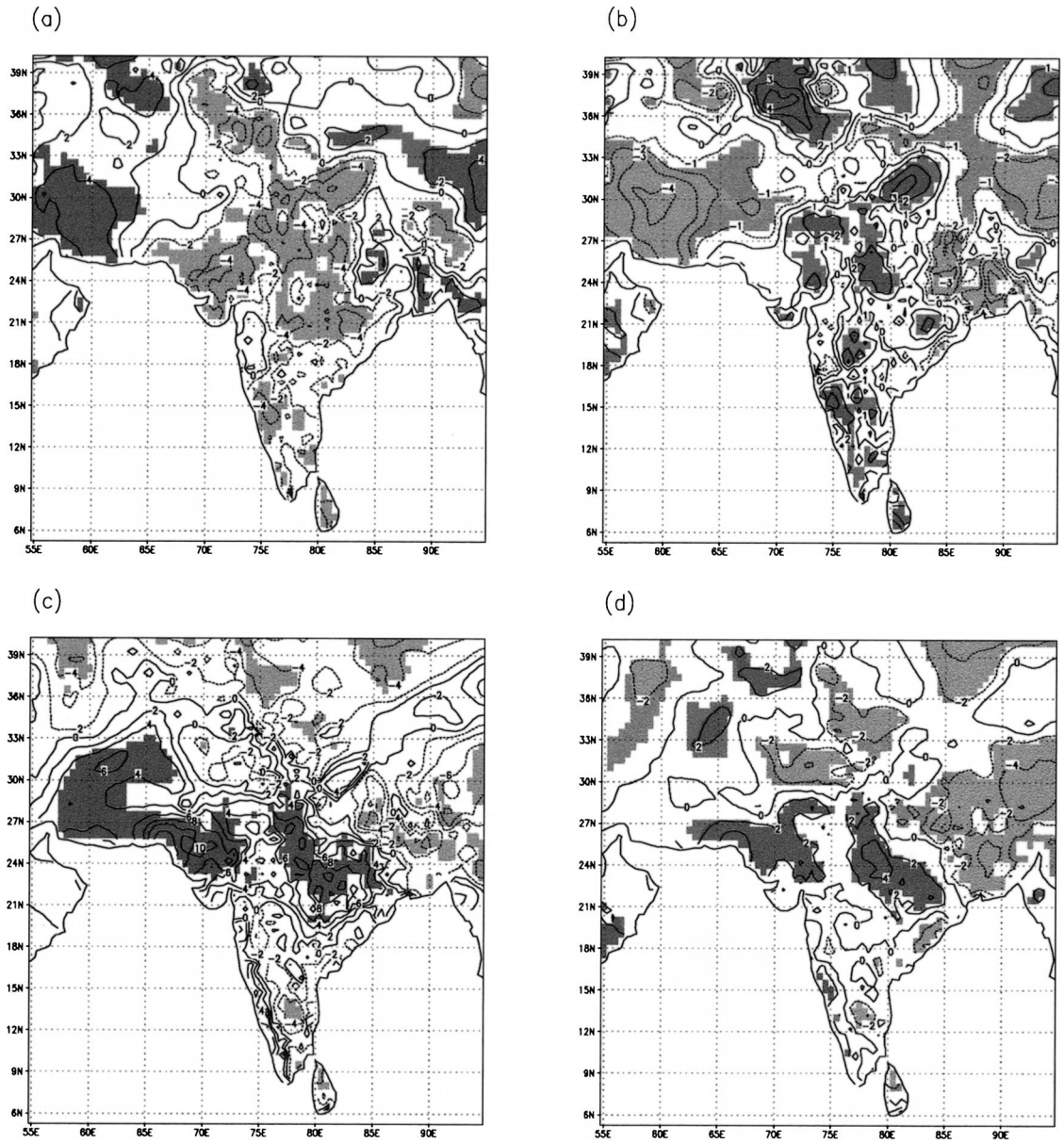

FIG. 2. Composite of the normalized ISMR anomaly distribution over (a) all El Niños between 1958 and 1997; (b) all El Niño years including those with positive IOD events minus that over pure El Niño years; and (c) pure positive IOD years. (d) As in (c) but for all positive IOD years including those that co-occurred with El Niños. Values significant at the 90% confidence level (from a two-tailed Student's *t* test) are shaded; positive (negative) significant values are shaded dark (light).

are found all over the Indian monsoon trough region, parts of central and southern India, regions north of the monsoon trough in the Indian region, Pakistan, and to the west of Pakistan; to a large extent, the distribution looks like a snapshot during an active monsoon period. Furthermore, the composite of the summer monsoon rainfall anomalies over the Indian region averaged over all the positive IOD events, including those that co-occurred with El Niño, between 1958 and 1997 (1961, 1963, 1967, 1972, 1977, 1982, 1983, 1994, and 1997) is presented in Fig. 2d. We can see positive anomalies of rainfall along the monsoon trough area, the west coast of India, northwest India, Pakistan, and farther north. Over the Indian region, the influence of the IOD is relatively more prominent throughout JJAS along the monsoon trough and the northwest region, in agreement with the mechanism proposed in the earlier study (Ashok et al. 2001). The magnitude of the surplus rainfall shown in this figure is, understandably, less than that shown in Fig. 2c, which showed rainfall anomalies during pure positive IOD years.

Figure 3a depicts the composite summer monsoon

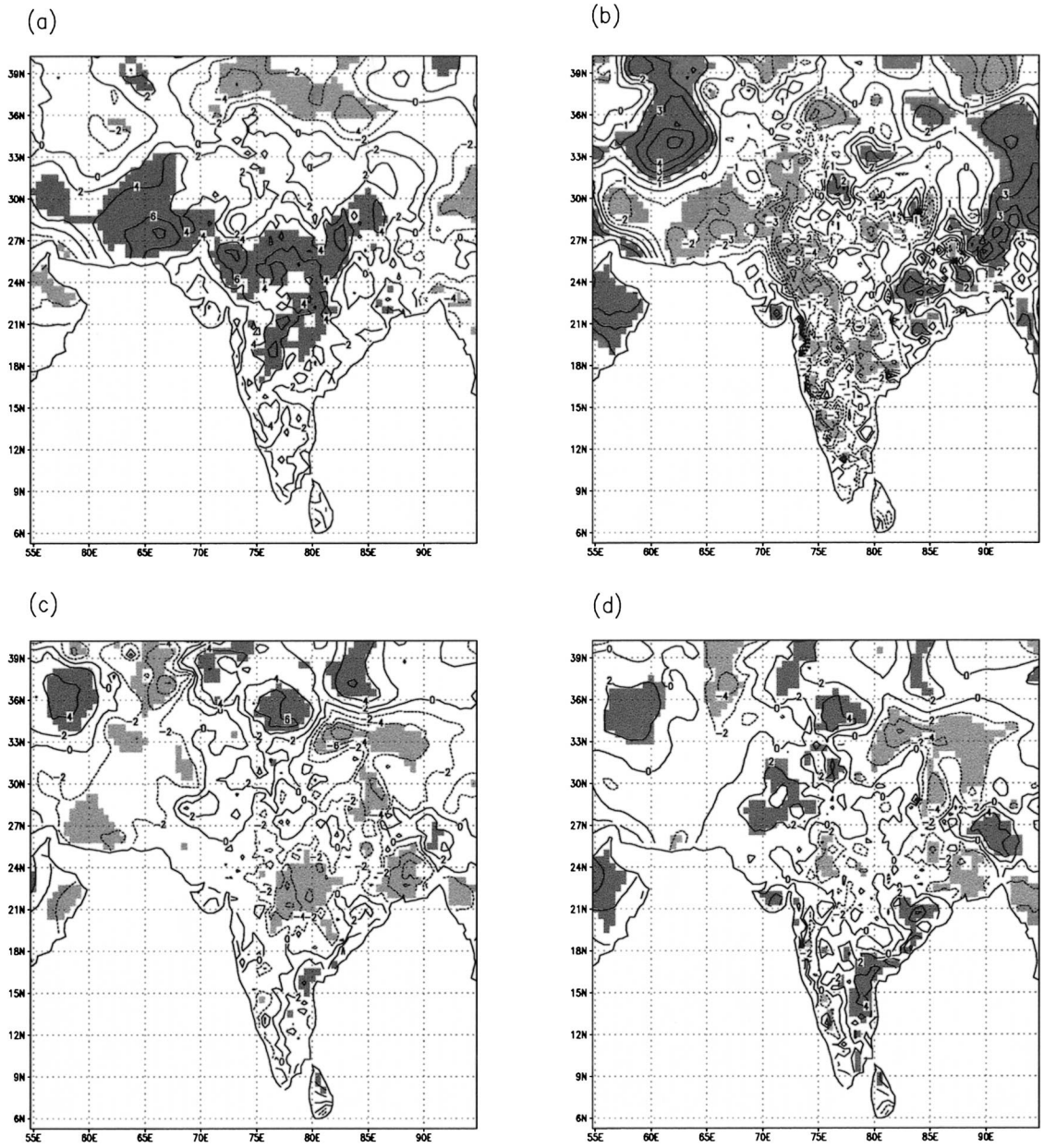

FIG. 3. Composite of the normalized ISMR anomaly distribution (a) over all La Niñas between 1958 and 1997; (b) over all the La Niña years including those with negative IOD events minus that over pure La Niñas; and (c) over pure negative IOD years. (d) As in (c) but for all negative IOD years including those that co-occurred with La Niñas. Values significant at the 90% confidence level (from a two-tailed Student's *t* test) are shaded; positive (negative) significant values are shaded dark (light).

rainfall anomaly distribution during pure La Niña years (1967, 1973, 1975, 1988, and 1999). Most of the Indian peninsula and monsoon trough regions receive surplus rainfall anomalies during these years. However, when the rainfall anomalies are averaged for those summers when the La Niña events co-occur with the negative IOD events, the La Niña–induced surplus rainfall anomalies are apparently reduced over large parts of peninsular, central, western, and northern Indian regions, as shown in Fig. 3b. The composite of the summer rainfall anomalies during pure negative IOD events (1958, 1960, 1989, 1992, and 1996) is shown in Fig. 3c. During the summers of these years, large parts of the monsoon trough region over India experience deficit rainfall. When the summer monsoon rainfall anomalies are averaged over all the negative IOD years, including those negative IOD events that co-occur with La Niña events (1958, 1960, 1964, 1970, 1989, 1992, and 1996), the deficit amounts are reduced, as indicated in the distribution of the difference (Fig. 3d).

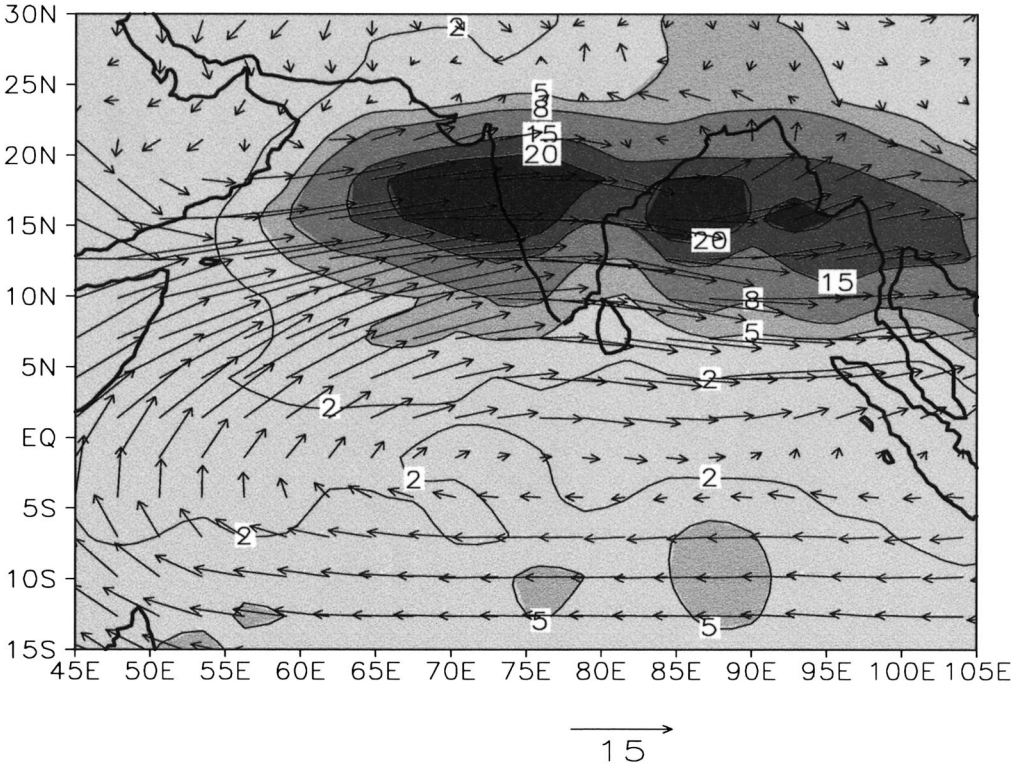

FIG. 4. Mean JJAS climatology of the FrAM1.0 AGCM obtained by averaging the outputs from the member ensembles of the control integration. Rainfall (mm day^{-1}) is shown in contours and 850-hPa wind (m s^{-1}) is in vectors.

Thus, while El Niño (positive IOD events) and La Niña (negative IOD events) have opposite impacts all over the Indian region through the JJAS season, the influences of the ENSO and the IOD on the monsoon rainfall are opposite to one another, as shown in Figs. 2 and 3.

b. General simulated features

In this subsection, we will present a brief description of the low-level circulation features of the mean Indian summer monsoon and the rainfall, obtained as an average of the five member ensembles of the control experiment. The simulated monsoon rainfall distribution is qualitatively realistic (Fig. 4), although the magnitude is higher than that from observations; simulated rainfall maxima centers over the Arabian Sea and the Bay of Bengal are realistic, given the relatively low resolution of the AGCM. The monsoon circulation at 850 hPa is reasonably well simulated. The simulated mean monsoon onset dates and the monsoon duration are realistic (not shown). For further details, refer to the relevant publications on the model performance (Guan et al. 2000, 2003).

The results from the IOD experiment are comparable to those of similar IOD experiments from our earlier study (Ashok et al. 2001). The simulated rainfall anomaly distribution from the positive IOD experiment indicates surplus rainfall along the monsoon trough area (not shown). The anomalous circulation originating off the coast of the Indonesian region crosses the equator and turns westward over the southeast Arabian Sea, thus reinforcing the low-level monsoon circulation around the monsoon trough. At 200 hPa, anomalous southbound wind flow originates from the Bay of Bengal region and converges over the cold eastern pole of the IOD (not shown). Intensification of the Tibetan anticyclonic circulation can also be seen. The simulated results are, in general, similar to our earlier studies (Ashok et al. 2001; Guan et al. 2003), and are in conformation with observations (Fig. 2c).

The simulated anomalies of the rainfall and wind at 850 hPa from the ENSO experiment are presented in Fig. 5a. A pronounced anomalous deficit in rainfall up to 35°N along with weakened monsoon circulation has been simulated over the Indian region, in agreement with the observations (see Fig. 2a); the simulated rainfall deficit center over western and central India is statistically significant (at the 90% significant level from a two-tailed *t* test). Surplus rainfall is simulated to the extreme south of India and farther south over the equatorial Indian Ocean. The distribution over the oceans is qualitatively similar to the observed rainfall pattern during summers of pure El Niño years, such as 1987, as

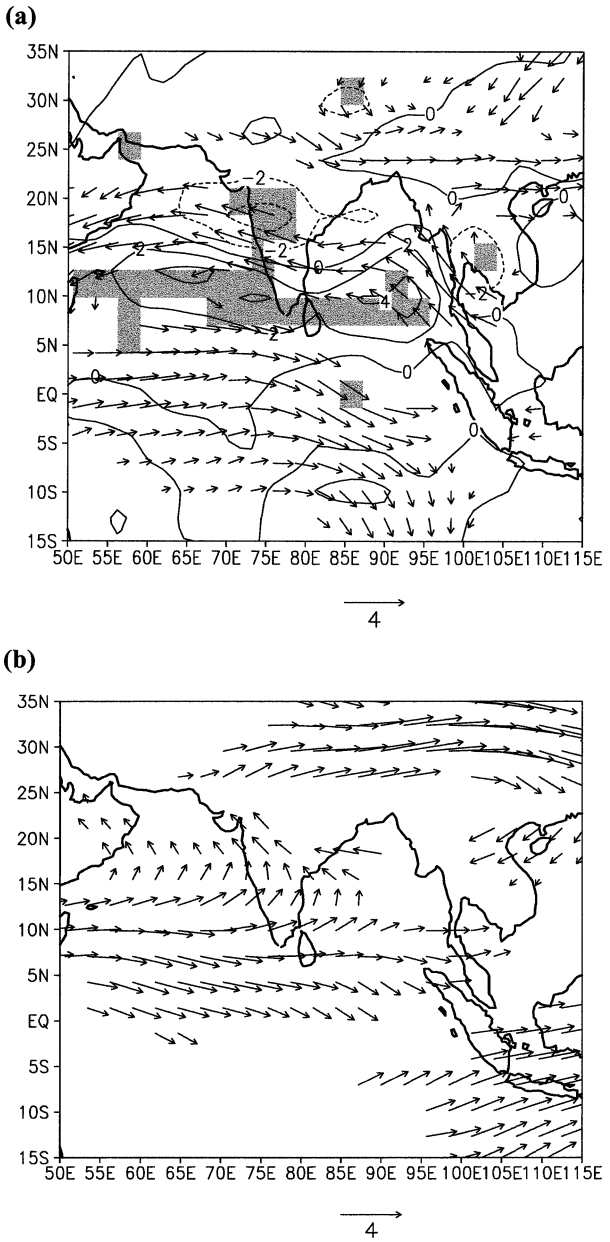

FIG. 5. (a) The JJAS rainfall (mm day^{-1}) and wind (m s^{-1}) anomalies at 850 hPa, as simulated in the ENSO experiment. Rainfall (wind) values significant at the 90% confidence level from a two-tailed student's *t* test are shaded (in vectors). (b) JJAS wind anomalies at 200 hPa, as simulated in the ENSO experiment. Note that only the significant winds are shown in (a) and (b).

we verified from the analysis of the assimilated observed rainfall data (Xie and Arkin 1996, figure not shown). These features agree with earlier ENSO–Indian monsoon simulation studies (e.g., Lau and Nath 2000). Some observational studies indicate that the shift of the Tibetan high to the east of its normal position causes break monsoon conditions and reduces the ISMR (Krishnamurti and Bhalme 1976; Pant and Kumar 1997). At 200 hPa, this shift of the Tibetan high is well simulated,

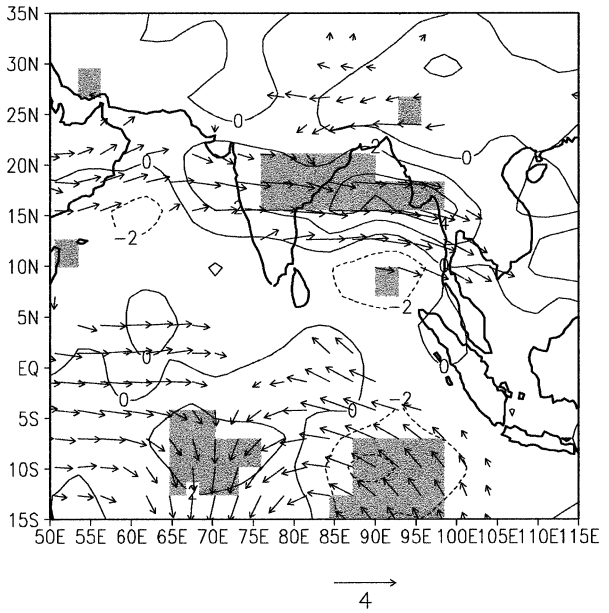

FIG. 6. As in Fig. 5a but for differences at 850 hPa (combined − ENSO).

with its center having moved to the east of its mean position (Fig. 5b). Our experiments confirm that El Niño weakens the Indian monsoon circulation at all levels and reduces the summer rainfall over India.

The difference in simulated rainfall and wind at 850 hPa between the combined and ENSO experiments is presented in Fig. 6. Within the Indian region, we can see a pronounced increase in rainfall all over the monsoon trough region, from Pakistan and the Gujarat region in western India extending into the Bay of Bengal. This shows that IOD-induced positive rainfall anomalies reduce the deficit rainfall due to ENSO. In the combined experiment, the monsoon circulation is much stronger around the monsoon trough compared to that in the ENSO experiment.

c. Maintenance of the circulation and moisture transport

The distribution of the velocity potential anomalies at 850 hPa as simulated in the ENSO experiment is presented in Fig. 7a. An anomalous center of divergence is located in the tropical west Pacific, flanked by a region of convergence anomaly to the west in the tropical Indian Ocean region, as observed.[7] The zone of convergence that is observed to the east of subtropical India

[7] Using the NCEP–NCAR reanalysis (Kalnay et al. 1996), we have composited the JJAS velocity potential anomalies for the pure El Niño years, 1965, 1969, 1976, 1986, 1987, and 1991. There is surface convergence at 850 hPa from equator–60°E extending south and northeast, with a baroclinic structure in the vertical (not shown). This convergence zone extends northeastward, via the eastern Bay of Bengal, all the way over to Myanmar and the south China region.

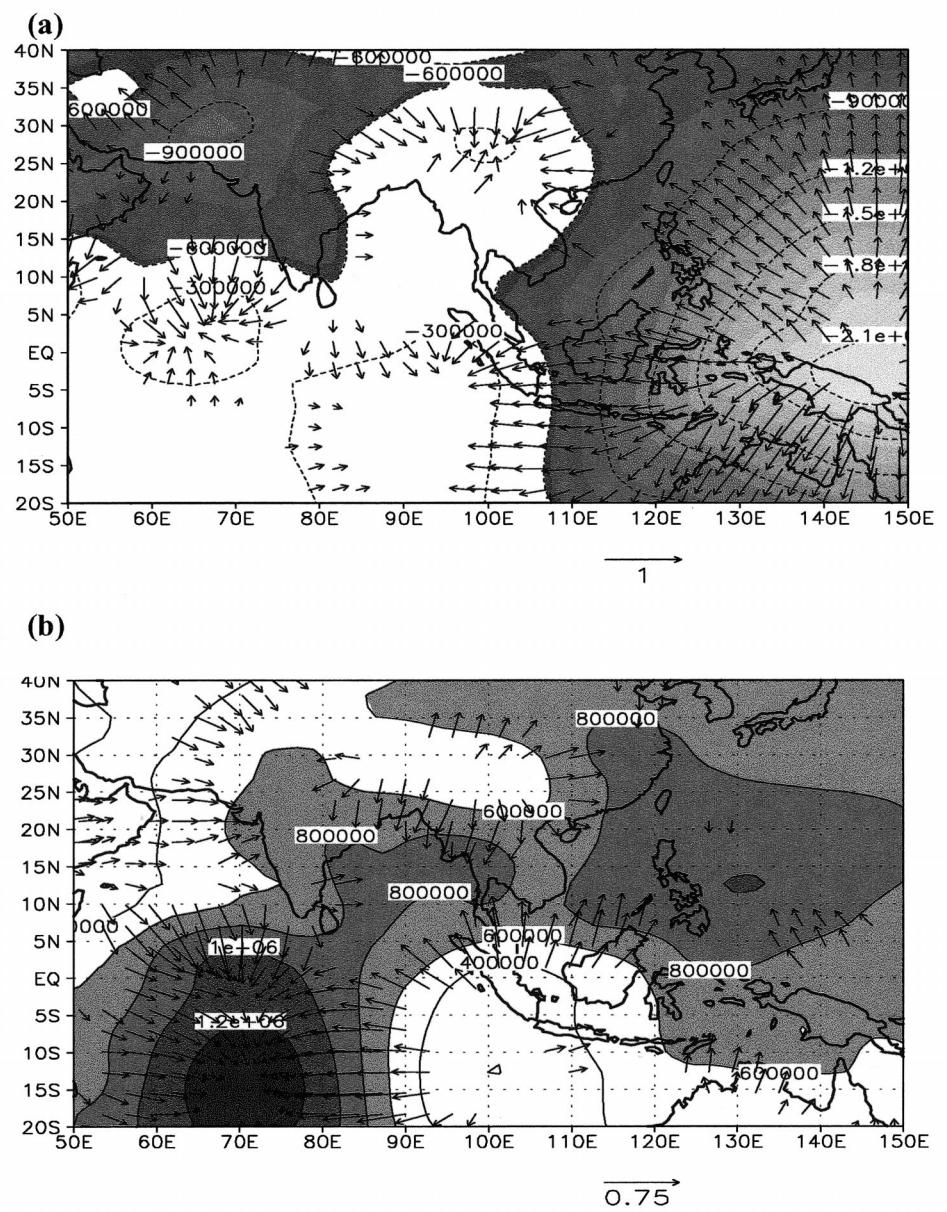

FIG. 7. (a) The 850-hPa JJAS velocity potential anomalies (contours; in $m^2\ s^{-1}$) and divergent winds (vectors; in $m\ s^{-1}$) as simulated in the ENSO experiment; (b) as in (a) but for the differences (combined − ENSO). Only the *significant* divergent wind anomalies (significant at the 90% confidence level from the two-tailed Student's *t* test) are shown at this level. Values less than $-60\ 000\ m^2\ s^{-1}$ in (a) and those less than $60\ 000\ m^2\ s^{-1}$ in (b) are shaded.

beyond 85°E is also well simulated, although the longitudinal position has shifted marginally westward. Because of this modulation of the Walker circulation, strong anomalous low-level divergence that causes the deficit rainfall is seen over the Indian region during the summers of pure El Niño years. The simulated ENSO response is, in general, baroclinic in the equatorial region, as indicated by the location of the convergence and divergence anomaly centers and the divergent wind anomalies at 200 hPa (not shown). Clearly, the El Niño type of SST has modified the Walker circulation over the tropical Indo–Pacific basin.

To understand how positive IOD events modulate the ENSO-induced circulation changes, the difference in the simulated velocity potential fields at 850 hPa between the combined and ENSO experiments is presented in Fig. 7b. In this figure, the divergence difference center can be seen over the Indian Ocean instead of over the west Pacific as simulated in the ENSO experiment. Specifically, it is located over the colder eastern pole region

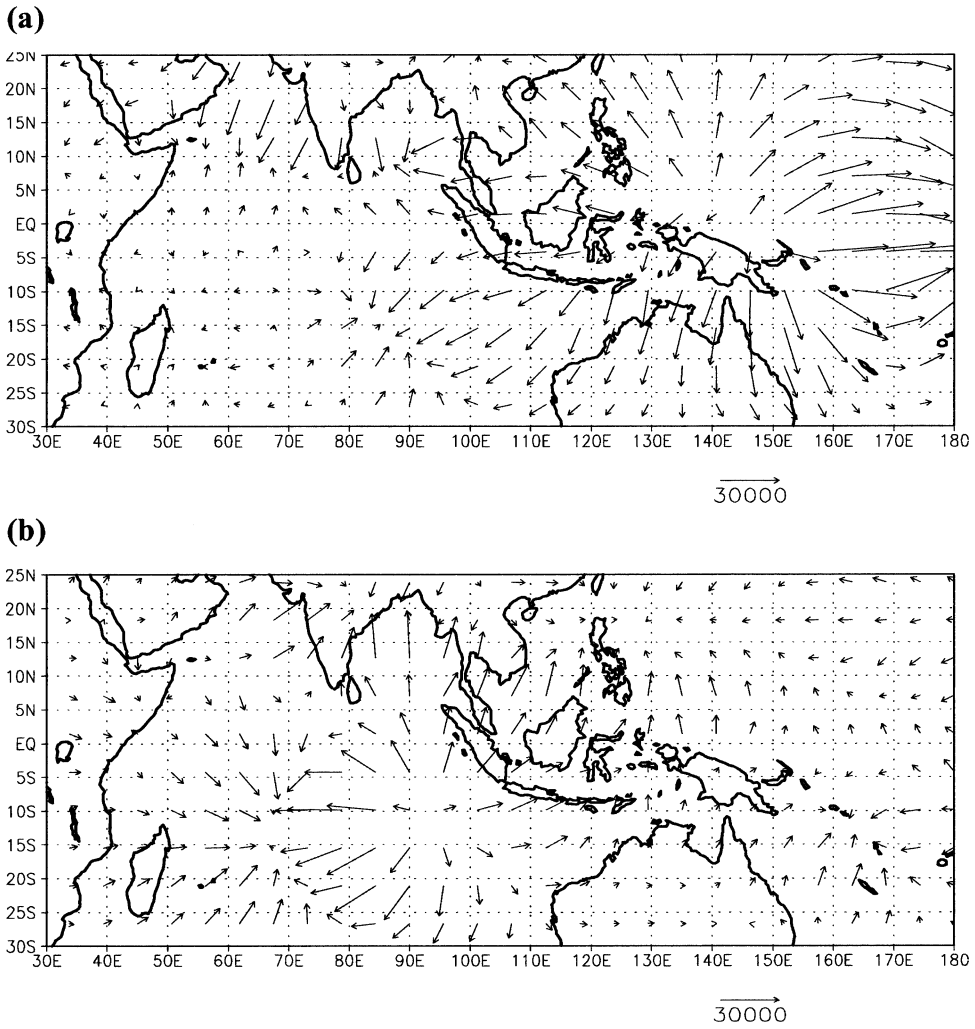

FIG. 8. Vertically integrated moisture flux (to be divided by 10 000; in kg m^{-1} s^{-1}) (a) anomalies as simulated in the ENSO experiment and (b) differences (combined − ENSO).

of the IOD. On the other hand, the convergence center over the western Indian Ocean that was simulated in the ENSO experiment has moved farther south in the combined experiment. The signature of the IOD can be clearly seen. There is a meridional component of divergence emanating off the coast of Indonesia, converging over the Bay of Bengal. In our earlier study in which the AGCM was forced with positive IOD anomalies (Ashok et al. 2001), we stressed the importance of the low-level meridional component of the divergence from the eastern pole that directly converges over the Bay of Bengal and monsoon trough. In the present combined experiment, apart from the aforementioned divergent meridional winds originating off the west coast of Indonesia, the anomalous convergence over India is also strengthened by winds beyond 15°N in the eastern Arabian Sea region. The vertical structure of the differences in the velocity potential between these two experiments is generally baroclinic, as evident from the 200-hPa distribution (not shown). The meridional component of the divergence at lower levels and convergence at the upper levels is relatively strong in the combined experiment, as compared to those simulated in the ENSO experiment.

The simulated anomalous moisture transports at different levels (not shown) are qualitatively similar to that of the anomalous velocity potential distributions shown in Fig. 7. The difference in the simulated moisture transport at 850 hPa between the combined experiment and the ENSO experiment indicates that the anomalous moisture divergence center has moved to the eastern Indian Ocean and is centered at the cold eastern pole of the IOD. There is much surplus moisture convergence over the warmer western pole region of the IOD as well as along the monsoon trough in the Indian region and over the Bay of Bengal.

The vertically integrated anomalous moisture flux simulated in the ENSO experiment is presented in Fig.

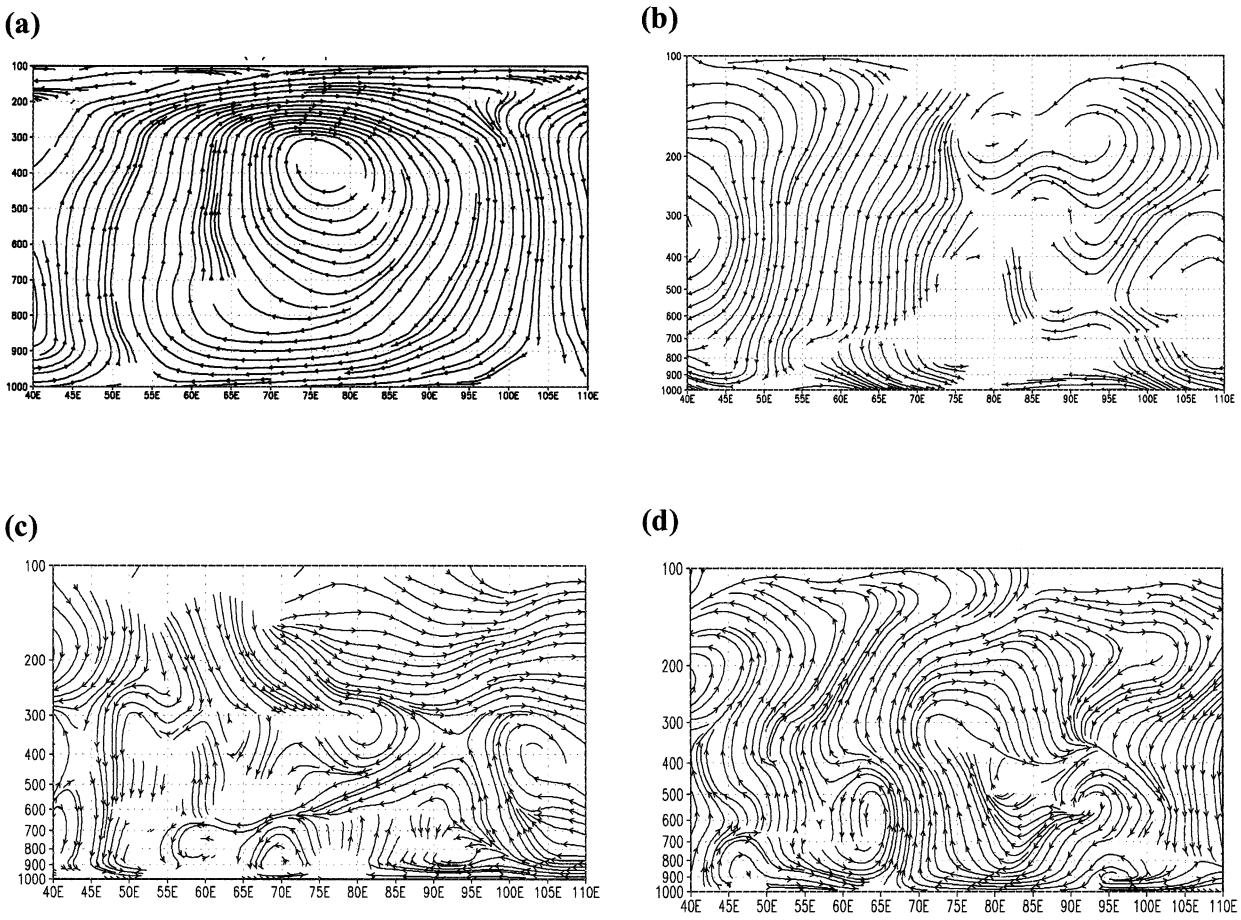

FIG. 9. The anomalous equatorial Walker circulation streamlines during JJAS (averaged over 10°S–5°N), derived from the NCEP nonrotating zonal component of the velocity and the vertical velocity: (a) composited over the pure positive IOD years 1961, 1967, and 1994 and (b) composited over the pure El Niño years 1969, 1987, and 1991. Simulated anomalous equatorial JJAS Walker circulation streamlines (averaged over 10°S–5°N): (c) in the ENSO experiment and (d) differences (combined − ENSO).

8a. There is a net divergence from the western Pacific area. Over the northern Indian Ocean, at about 7°N, there is moisture convergence parallel to the monsoon trough over India, suggesting that the moisture over the Indian region may have anomalously shifted south. There is net divergence of moisture flux toward the south over the Indian region. The difference in the vertically integrated anomalous moisture flux at 850 hPa between the combined experiment and ENSO experiment is presented in Fig. 8b. The difference distribution now shows a prominent moisture divergence center to the west of the Indonesian coast, flanked by a moisture convergence center to the west. This anomalous moisture convergence center in the western tropical Indian Ocean causes anomalous divergence of moisture a little farther north up to about 15°N; this anomalous divergence in turn induces anomalous convergence farther to the north over the Gujarat and adjoining regions. In the Indian region, net moisture convergence is simulated in the vertically integrated moisture difference distribution over the monsoon trough region over India and the head of the Bay of Bengal. Our simulations confirm that the IOD can compensate for the ENSO effect over the Indian region, while over places like Indonesia, it amplifies the ENSO influence by causing further loss in moisture that accentuates the dryness.

d. Walker and Hadley circulation anomalies

ENSO modulates the Walker and Hadley circulations in the Tropics. A co-occurring IOD event in turn modulates the ENSO influences (and vice versa). In this subsection, we study these circulation changes in the equatorial vertical plane of the Indian Ocean sector, from observations as well as from simulations carried out in this study.

During the summer monsoon season of the pure positive IOD years (such as 1961, 1967, and 1994), a strong well-defined *single* Walker cell can be seen over the equatorial Indian Ocean, with descending motion in the east and ascending motion in the west (not shown). The composited Walker circulation obtained by averaging

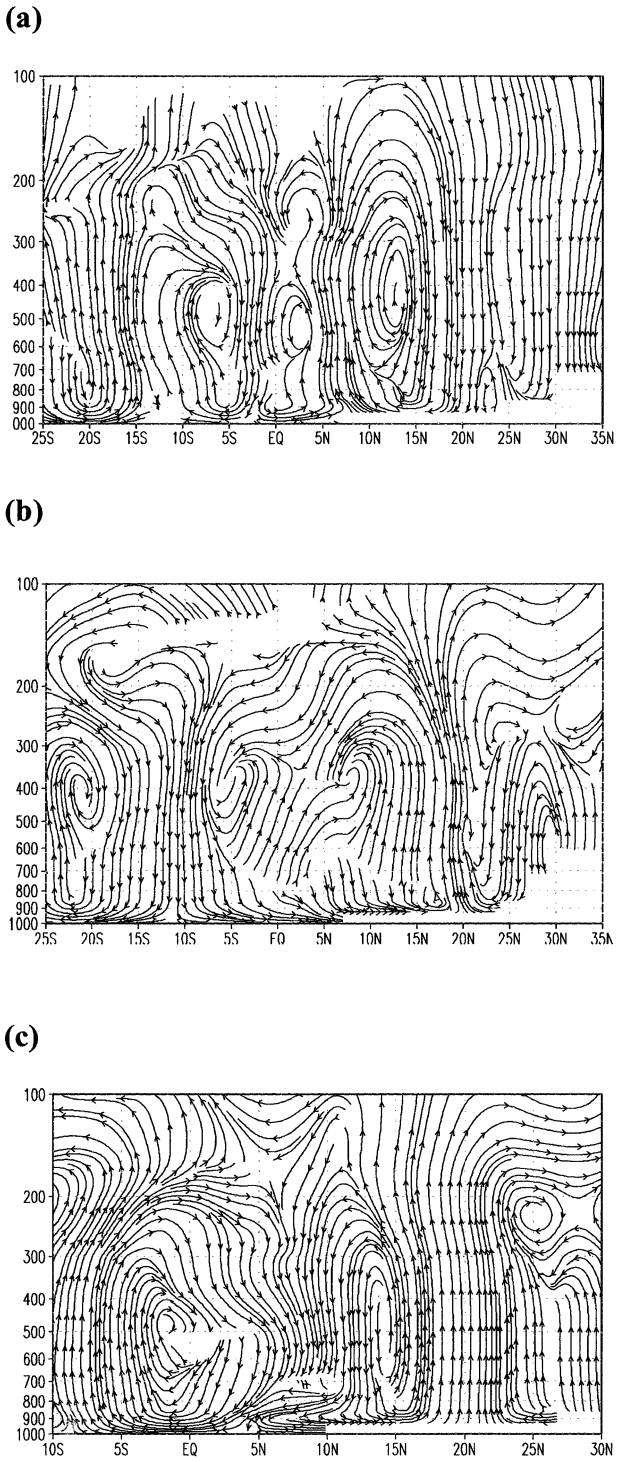

FIG. 10. Anomalous JJAS Hadley circulation streamlines (a) simulated in the ENSO experiment (zonally averaged over 70°–85°E) and (b) differences (combined − ENSO) zonally averaged over 80°–95°E. (c) As in (b) but zonally averaged over 65°–75°E. Orography mask has been applied in all figures.

the Walker circulation during these summers also confirms this fact (Fig. 9a). Over the Pacific, the Walker circulation is either two-celled, as in 1961, or very disorganized, as in 1967 and 1994 (not shown). In contrast, during the same season of the pure El Niño years (without any IOD events) such as 1969, 1987, and 1991, relatively diffused, *incomplete* zonal circulation patches, with many interannual variations, are observed over the equatorial Indian Ocean (not shown); the composite of the circulation during these years also shows a very diffused Walker circulation over the tropical Indian Ocean (Fig. 9b). The vertical direction of these Walker circulation anomalies over the tropical Indian sector is very different in each of the aforementioned El Niño years. A *single* strong Walker cell with *descending* motion in the *east* and *ascending* motion in the *west* can be seen over the equatorial Indian Ocean during an El Niño event only when a *positive* IOD event co-occurs, such as in 1997 (not shown). This feature of the IOD is consistent with strong surface divergent easterly winds over the equatorial Indian Ocean during the positive IOD events; such *strong surface easterlies over the equatorial Indian Ocean* cannot be found in the aforementioned *pure* ENSO years. This difference in Walker circulation anomalies persists even in September–November (Ashok et al. 2003a).

The equatorial Walker circulation anomalies simulated in the ENSO experiment indicate anomalous subsidence over the equatorial Pacific region between 100° and 165°E and upward motion farther east, as observed (not shown). Over most of the Indian Ocean region, the Walker circulation anomaly direction is not well defined (Fig. 9c). The circulation is diffused, in agreement with the observations; there is no single Walker cell covering a large area of the tropical Indian Ocean basin. The difference in the simulated equatorial Walker circulation between the combined experiment and the ENSO experiment is presented in Fig. 9d. From this figure, ascending motion can be clearly seen over the western pole of the IOD, and descending motion over the eastern pole. This indicates that in the combined experiment, there is excess subsidence (upward motion) over the eastern (western) pole of the IOD region as compared to that in the ENSO experiment, completing a *single* Walker cell over the Indian Ocean and *separate* from any *anomalous* Walker cells over the western Pacific.

The description of the simulated Walker circulation anomalies from the different experiments presented above conforms to our earlier discussion of simulated velocity potential anomalies (see Fig. 7).

In Fig. 10a, we present the simulated anomalous Hadley circulation from the ENSO experiment, averaged between 70° and 85°E. To the north of the equator, there is rising motion to 13°N, beyond which we can find anomalous subsidence over the monsoon trough area and farther north, resulting in the reduction of convection and rainfall over India.

As the IOD comprises two SSTA poles, we expect

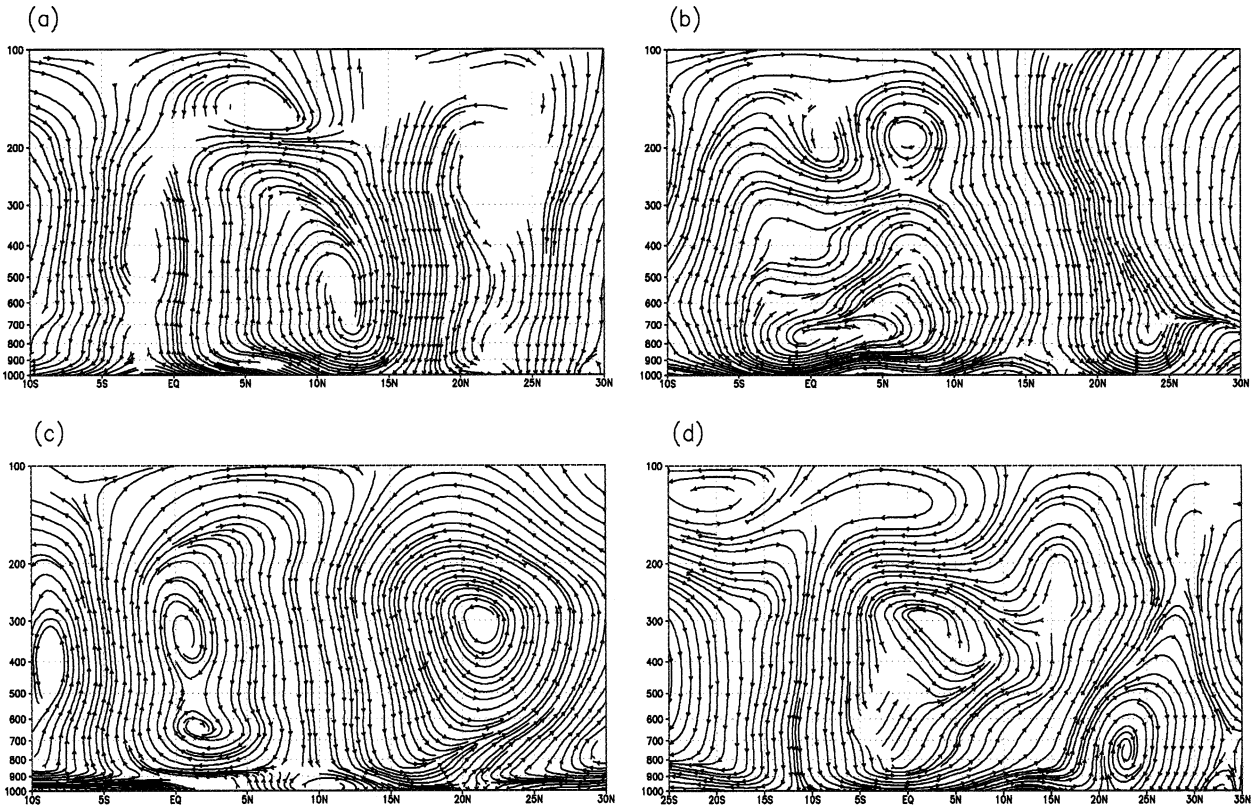

FIG. 11. NCEP anomalous JJAS Hadley circulation streamlines zonally averaged (a) over 70°–85°E during 1969, (b) 70°–85°E during 1987, (c) 65°–75°E during 1994, and (d) 80°–95°E during 1994.

that the mechanisms by which each of these poles may influence the ENSO–monsoon relationship may be different from one another. To examine this, we first study the difference of the Hadley circulation between the ENSO and combined experiments over the eastern pole. The difference from the combination experiment averaged over 80°–95°E is presented in Fig. 10b. There is excess subsidence to the south of the equator at about 12°S in the combined experiment. Part of this anomalously subsiding wind crosses the equator and rises upward beyond 17°N. Ascending motion can be seen to about 23°N. The IOD-induced Hadley circulation cell extends from about 5°S to 23°N and brings moisture from the south into the monsoon trough region. Thus, the IOD-induced Hadley circulation can compensate for the descending motion induced by the ENSO forcing and lessen the latter's influence on the Indian monsoon.

To understand the role of the warmer western pole of the positive IOD in reducing the El Niño influence on the Indian monsoon, we show the difference in the simulated Hadley circulation between the combined and ENSO experiments averaged between 65° and 75°E (Fig. 10c). The anomalous excess ascending motion over the warm pole between 10°S and the equator induces anomalous subsidence northward to 15°N, which in turn triggers ascending motion farther north, causing surplus rainfall over the northwestern part of the monsoon trough as well as the coast of India and Pakistan, etc.

The corresponding observed Hadley circulation anomalies during the summer seasons of the pure ENSO years of 1969 and 1987 and the pure IOD year of 1994 are presented as examples in Fig. 11. These can be explained by the aforementioned simulated Hadley circulation anomalies shown in Fig. 10.

Figures 10b and 10c demonstrate that both poles of the positive IOD SSTA in the Indian Ocean can reduce the ENSO-induced subsidence over the Indian region when these events co-occur.

4. Discussion and conclusions

This paper examines the relative influences of ENSO and the IOD events on the ISMR using observational analysis and results from experiments. Composite analysis of the Indian summer monsoon rainfall anomalies during the pure IOD years, pure ENSO years, and co-occurring years carried out in this study shows that positive (negative) IOD significantly reduces the impact of the El Niño (La Niña) on the Indian monsoon, confirming the hypothesis put forward in an earlier paper (Ashok et al. 2001).

We conducted several multiensemble sensitivity experiments using an AGCM with various types of SST fields as lower boundary forcing to assess the influence of the El Niño, the IOD, and their combined influence on the ISMR and related circulation. The conclusions from these experiments are as follows.

When an El Niño occurs, it induces an anomalous divergence center over the equatorial western Pacific at lower levels with a baroclinic structure in the vertical. This low-level anomalous divergence center induces an anomalous convergence center to the west, resulting in a single anomalous Walker cell ascending in the western tropical Indian Ocean and descending over the western Pacific. This anomalous convergence center in the Indian Ocean and the anomalous convergence center to the northeast over southern China and Myanmar are complemented by the anomalous surface divergence over the Indian monsoon region that causes weakened summer monsoon rainfall over India. Over the tropical Indian Ocean, during the summers of pure El Niño years, the Walker circulation is diffuse and weak.

Whenever these two ocean processes occur together, the low-level western Pacific divergence center that occurs during a pure El Niño is weakened and a new anomalous divergence center, relative to the pure El Niño year, is induced off the west coast of Indonesia. This forms an *anomalous Walker cell* over the IOD region s*eparate* from the Walker circulation over the Pacific. The divergent wind in the east results in intensification of cross-equatorial Hadley circulation, resulting in anomalously surplus ISMR, as in years such as 1997, when both ocean phenomena co-occurred.

When the positive IOD event occurs, both poles of the IOD contribute to the surplus rainfall over India and thereby reduce the ENSO influence. Our AGCM experiments also demonstrate that positive IOD events amplify the ENSO-induced subsidence and deficit rainfall over the Indonesian region. The net combined influence of these ocean processes depends on the relative phases and strengths, as mentioned in our earlier study (Ashok et al. 2001). The fact that the IOD has apparently weakened the ENSO–monsoon relationship (Ashok et al. 2001) makes the IODMI a potentially useful predictor for the Indian summer monsoon rainfall.

Acknowledgments. This paper is dedicated to the memory of the late Dr. M. K. Soman, a well-known monsoon researcher from IITM, India, who passed away at a young age. The authors thank Pascal Delecluse and D. V. Bhaskar Rao for their helpful discussions during the course of this work. The authors are grateful to two anonymous reviewers and Martin P. Hoerling for useful comments that improved the earlier version of the manuscript. The figures presented in this work have been prepared using the GrADS software.

REFERENCES

Ashok, K., Z. Guan, and T. Yamagata, 2001: Impact of the Indian Ocean Dipole on the relationship between the Indian Monsoon rainfall and ENSO. *Geophys. Res. Lett.,* **26,** 4499–4502.

——, ——, and ——, 2003a: A look at the relationship between the ENSO and the Indian Ocean dipole. *J. Meteor. Soc. Japan,* **81,** 41–56.

——, ——, and ——, 2003b: Influence of the Indian Ocean dipole on the Australian winter rainfall. *Geophys. Res. Lett.,* **30,** 1821, doi:10.1029/2003GL017926.

Behera, S. K., R. Krishnan, and T. Yamagata, 1999: Unusual ocean–atmosphere conditions in the tropical Indian Ocean during 1994. *Geophys. Res. Lett.,* **26,** 3001–3004.

Guan, Z., S. Iizuka, M. Chiba, S. Yamane, K. Ashok, and T. Yamagata, 2000: Frontier Atmospheric General Circulation Model version 1.0 (FrAM 1.0): Model climatology. FRSGC Tech. Rep. FTR-1, Yokohama, Japan, 27 pp.

——, K. Ashok, and T. Yamagata, 2003: Summertime response of the tropical atmosphere to the Indian Ocean sea surface temperature anomalies. *J. Meteor. Soc. Japan,* **81,** 533–561.

Kalnay, E., and Coauthors, 1996: The NCEP/NCAR 40-Year Reanalysis Project. *Bull. Amer. Meteor. Soc.,* **77,** 437–471.

Klenk, K. F., P. K. Bhartia, E. Hilsenrath, and A. J. Fleig, 1983: Standard ozone profile from balloon and satellite data sets. *J. Climate Appl. Meteor.,* **22,** 2012–2022.

Kripalani, R. H., and A. Kulkarni, 1999: Climatological impact of El Niña on the Indian monsoon: A new perspective. *Weather,* **52,** 39–46.

Krishna Kumar, K., M. K. Soman, and K. Rupa Kumar, 1995: Seasonal forecasting of Indian summer monsoon rainfall. *Weather,* **50,** 449–467.

——, B. Rajagopalan, and M. A. Cane, 1999: On the weakening relationship between the Indian monsoon and ENSO. *Science,* **284,** 2156–2159.

Krishnamurti, T. N., and H. N. Bhalme, 1976: Oscillations of a monsoon system. Part I: Observational aspects. *J. Atmos. Sci.,* **33,** 1937–1954.

Kuo, H. L., 1974: Further studies of the parameterization of the influence of cumulus convection on large-scale flow. *J. Atmos. Sci.,* **31,** 1232–1240.

Laprise, R., and C. Girard, 1990: A spectral general circulation model using a piecewise-constant finite-element representation on a hybrid vertical coordinate system. *J. Climate,* **3,** 32–52.

Lau, N.-C., and M. J. Nath, 2000: Impact of ENSO on the variability of the Asian–Australian monsoon as simulated in GCM experiments. *J. Climate,* **13,** 4287–4309.

Legates, D. R., and C. J. Willmott, 1990: Mean seasonal and spatial variability in gauge-corrected global precipitation. *Int. J. Climatol.,* **10,** 111–127.

Mellor, G. L., and T. Yamada, 1974: An hierarchy of turbulence closure models for planetary boundary layers. *J. Atmos. Sci.,* **31,** 1791–1806.

Palmer, T. N., G. J. Shutts, and R. Swinbank, 1986: Alleviation of systematic westerly bias in general circulation and numerical weather predication models through an orographic gravity wave drag parameterization. *Quart. J. Roy. Meteor. Soc.,* **112,** 1001–1039.

Pant, G. B., and K. Rupa Kumar, 1997: *Climates of South Asia.* J. Wiley and Sons, 317 pp.

Parthasarathy, B., K. Rupa Kumar, and A. A. Munot, 1993: Homogeneous Indian monsoon rainfall: Variability and prediction. *Proc. Indian Acad. Sci.,* **102,** 121–155.

Rao, A. S., S. K. Behera, Y. Masumoto, and T. Yamagata, 2002: Interannual subsurface variability in the tropical Indian Ocean with special emphasis on the Indian Ocean dipole. *Deep-Sea Res.,* **49B,** 1549–1572.

Rao, Y. P., 1976: *Southwest Monsoon. Meteor. Monogr.,* Synoptic Meteorology 1/1976, India Meteorological Department, 367 pp.

Rayner, N. A., E. B. Horton, D. E. Parker, C. K. Folland, and R. B.

Hackett, 1996: Version 2.2 of the global sea ice and surface temperature data set, 1903–1994. Climate Research Tech. Note 74, Hadley Centre for Climate Prediction and Research, Met Office, 35 pp.

Saji, N. H., B. N. Goswami, P. N. Vinayachandran, and T. Yamagata, 1999: A dipole mode in the tropical Indian Ocean. *Nature,* **401,** 360–363.

Shibata, K., 1989: An economical scheme for the vertical integral of atmospheric emission in long wave radiation transfer. *J. Meteor. Soc. Japan,* **67,** 1047–1055.

——, and T. Aoki, 1989: An infrared radiative scheme for the numerical models of weather and climate. *J. Geophys. Res.,* **94,** 14 923–14 943.

Viterbo, P., and A. C. M. Beljaars, 1995: An improved land surface parameterization scheme in the ECMWF model and its validation. *J. Climate,* **6,** 777–795.

Webster, P. J., V. O. Magana, T. N. Palmer, J. Shukla, R. A. Tomas, M. Yanai, and T. Yasunari, 1998: Monsoons: Processes, predictability, and prospects for prediction. *J. Geophys. Res.,* **103** (C7), 14 451–14 510.

——, A. Moore, J. Loschnigg, and M. Leban, 1999: Coupled dynamics in the Indian Ocean during 1997–1998. *Nature,* **401,** 356–360.

Willmott, C. J., and K. Matsuura, 1995: Smart interpolation of annually averaged air temperature in the United States. *J. Appl. Meteor.,* **34,** 2557–2586.

Xie, P., and P. A. Arkin, 1996: Analyses of global monthly precipitation using gauge observations, satellite estimates, and numerical model predictions. *J. Climate,* **9,** 840–858.

Yamagata, T., S. K. Behera, S. A. Rao, Z. Guan, K. Ashok, and H. N. Saji, 2003: Comments on ''Dipoles, temperature gradients, and tropical climate anomalies.'' *Bull. Amer. Meteor. Soc.,* **84,** 1418–1421.